



HAL
open science

Did the Flores backarc thrust rupture offshore during the 2018 Lombok earthquake sequence in Indonesia?

Xiaodong Yang, Satish C. Singh, Anand Tripathi

► To cite this version:

Xiaodong Yang, Satish C. Singh, Anand Tripathi. Did the Flores backarc thrust rupture offshore during the 2018 Lombok earthquake sequence in Indonesia?. *Geophysical Journal International*, 2020, 221, pp.758-768. 10.1093/gji/ggaa018 . insu-03748812

HAL Id: insu-03748812

<https://insu.hal.science/insu-03748812>

Submitted on 16 Mar 2023

HAL is a multi-disciplinary open access archive for the deposit and dissemination of scientific research documents, whether they are published or not. The documents may come from teaching and research institutions in France or abroad, or from public or private research centers.

L'archive ouverte pluridisciplinaire **HAL**, est destinée au dépôt et à la diffusion de documents scientifiques de niveau recherche, publiés ou non, émanant des établissements d'enseignement et de recherche français ou étrangers, des laboratoires publics ou privés.

Did the Flores backarc thrust rupture offshore during the 2018 Lombok earthquake sequence in Indonesia?

Xiaodong Yang,¹ Satish C. Singh^{1,2} and Anand Tripathi¹

¹Laboratoire de Géoscience Marine, Institut de Physique du Globe de Paris, 1 rue Jussieu, 75238 Paris Cedex 05, France. E-mail: yang@ipgp.fr

²Earth Observatory of Singapore, Nanyang Technological University, 50 Nanyang Avenue, Singapore

Accepted 2020 January 6. Received 2020 January 3; in original form 2019 September 2

SUMMARY

The Flores thrust forms the west segment (~450 km) of a very active, ~E–W striking, ~800-km-long backarc thrust along the east Sunda Arc. In 2018, a deadly earthquake sequence composed of ~110 M_4+ events rattled the Indonesian island of Lombok near the Flores thrust and caused tremendous damage on the island, however what is the nature of rupturing during this earthquake sequence remains unknown. Here, using a total of 2120 km of high-resolution seismic profiles covering ~300 km of the Flores thrust off Bali, Lombok and Sumbawa, in addition to earthquake data and InSAR measurements, we investigated the active thrusting during this earthquake sequence. Our seismic interpretation and structural mapping show that offshore north of Lombok and Bali, the remarkable Flores thrust is essentially blind, deforming the seabed by folds, not faults. The Lombok earthquakes were all shallow thrust events with depth <40 km and occurred within ~35 km north of the Rinjani volcano beneath the Lombok Island and its northern extremity. The InSAR measurements suggested that the most of the crustal deformation caused by these earthquakes occurred the north the and northeast of the island. The maximum vertical deformation was ~36 cm near the northwest margin of the island, caused by the 5th August M_w 6.9 event. These observations combined with the presence of blind thrusts off Lombok suggest that the offshore portion of Flores thrust did not rupture during the 2018 Lombok earthquake sequence; the most coseismic slip must have occurred along a deep-rooted, north-verging basal fault and a range of imbricate thrusts beneath the north of the island, not along the buried thrusts offshore. Despite being blind off Lombok and Bali, the Flores thrust can still pose tsunami threats to the adjacent population centres by rupturing the seafloor during future large earthquakes ($M > 7$) that occur directly on the offshore blind thrusts, not beneath the island like the Lombok sequence. The proximity of the Rinjani volcano and thrust earthquakes suggests a possible role of volcanic activity (e.g. magmatic fluids and gas migration, stress change induced by pressurized magma chamber) in inducing the Lombok earthquakes.

Key words: Seismicity and tectonics; Backarc basin processes; Crustal structure; Tsunamis; Volcanic hazards and risks.

1 INTRODUCTION

In 2018, a deadly earthquake sequence struck the Indonesian island of Lombok, causing significant casualties (>550) and tremendous damage on the island. The earthquake sequence began with a M_w 6.4 event on 28th July followed by 110 events with magnitude (M) > 4 until 19th August (USGS earthquake catalogue). Among all events, four large earthquakes with $M_w > 6$ were recorded: 28th July M_w 6.4, 5th August M_w 6.9, 19th August M_w 6.3 and 19th August M_w 6.9.

These earthquakes appear to essentially occur along the Flores backarc thrust beneath the Lombok Island along the east Sunda

arc, Indonesia. The Flores backthrust north of the island arc (i.e. Bali, Lombok, Sumbawa, Flores Sumba, Rote and Timor) has developed due to the northward subduction of the Indo-Australian oceanic plate beneath the Eurasian plate (Fig. 1a, Hamilton 1979; Hall & Spakman 2015) at 70 ± 1.0 mm yr⁻¹ west of Lombok and the collision of the Australian continent with the west Banda arc at 33 ± 0.9 mm yr⁻¹ south of Rote Island (Koulali *et al.* 2016). Unlike the other backthrusts observed in the forearc region along the Andaman–Sumatra segment of the Sunda arc (Chauhan *et al.* 2009; Singh *et al.* 2010, 2013; Mukti *et al.* 2012), the Flores backthrust lies in the backarc region. Early marine geophysical investigation suggested that the backthrust extends from the Bali basin towards

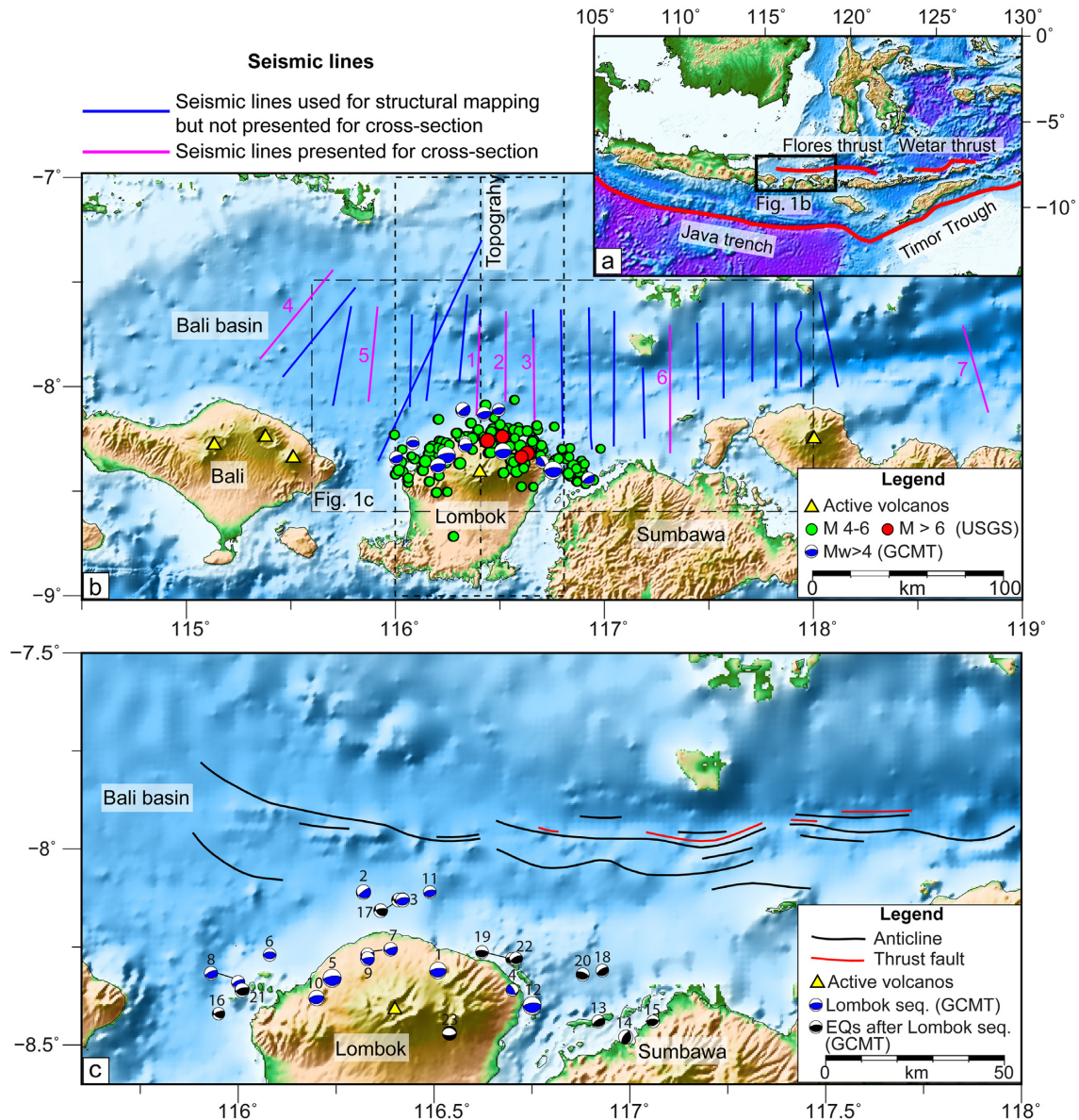


Figure 1. Regional map of study area, east Indonesia. (a) Primary tectonic elements in the Sunda arc-continent collision, major faults (thick red lines) (Hamilton 1979). Topography and bathymetry are from Global ocean & land terrain models (<https://www.gebco.net>). (b) Seismotectonic setting of the Lombok earthquake sequence. Location of volcanoes is from Global Volcanism Program, Smithsonian Institution. Seismicity is from USGS earthquake catalogue <https://earthquake.usgs.gov/earthquakes/>. Green dots correspond to earthquakes of M 4–6, red dots correspond to earthquakes with M 6+. Focal mechanisms are from Global Centroid Moment Tensor (GCMT) catalogue. Seismic profiles are 2-D marine reflective seismic data, which are all used for detailed structural mapping, amongst which seven lines (i.e. purple lines) are presented for cross-section view. (c) Structural map of the Flores thrust, off Bali, Lombok and Sumbawa. GCMT focal mechanisms are used for both the Lombok sequence (blue) and the earthquakes that followed (black), which are all numbered according to the occurrence time.

Wetar, consisting of two segments: the 450-km-long Flores thrust and the 350-km-long Wetar thrust (Fig. 1a, Hamilton 1979; Usna *et al.* 1979; Silver *et al.* 1983), whereas a recent geodetic study argues that it extends for 2000 km all the way from East Java to north of Timor (Koulali *et al.* 2016). Uncertainties remain as to what extent the Flores thrust deforms the backarc region. This remarkable backthrust is complicated in structural style, expressed by a deep-rooted main basal fault and a series of overlying imbricate thrusts and associated folds (Silver *et al.* 1983, 1986; Breen *et al.* 1989). It is very active and has produced ~25 M 6+ earthquakes since 1960 before the Lombok sequence (Ekström *et al.* 2012; USGS catalogue), among which the 1992 M_w 7.9 Flores earthquake is the

largest event, rupturing offshore and generating a large, destructive tsunami (Beckers & Lay 1995).

The origin of this backarc thrust has been attributed to several processes: reversal of subduction polarity (Hamilton 1979); stress propagation through the arc (Silver *et al.* 1983); magmatic intrusion in the arc (Hamilton 1979); gravitational sliding or spreading in the backarc (Hamilton 1979; Breen *et al.* 1989); and stress transfer across the rigid arc-block (ten Brink *et al.* 2009), but no general agreement exists as to its cause. Recent geodetic results suggest that it is linked to the subduction zone by two NNE-trending strike-slip faults and plays a distinct role in strain partitioning between the subducting Indo-Australian Plate and the overriding Sunda

Block with relative motions from $6 \pm 1.0 \text{ mm yr}^{-1}$ in East Java to $26 \pm 1.0 \text{ mm yr}^{-1}$ near Flores Island, $28 \pm 1.7 \text{ mm yr}^{-1}$ near Wetar Island (Koulali *et al.* 2016). However, as an important regional structure, its precise nature of thrusting remains unclear. In this study, we focus on its western segment, the Flores backthrust, to investigate its active thrusting and structural deformation in the light of the recent Lombok earthquake sequence (Fig. 1).

Just south of these earthquakes, the active volcano Rinjani on Lombok Island (Figs 1b and c, Foden 1983) lies $\sim 170 \text{ km}$ above the Benioff zone (e.g. Hutchison 1976; Lüschen *et al.* 2011). Its AD 1257 Samalas eruption is identified as the source of the largest sulphate peak recorded in polar ice cores (Lavigne *et al.* 2013) over the last 2.3 kyr (Sigl *et al.* 2014) and may have been the most powerful volcanic blast in the Common Era (Vidal *et al.* 2015).

The presence of the Rinjani volcano in the vicinity of the Flores thrust, and the large-magnitude of the Lombok earthquakes poses the question ‘are there any links between these features?’. To address this question, we carried out a comprehensive investigation into the Lombok seismicity using high-resolution seismic profiles, earthquake data and InSAR measurements. In this paper, we (1) map the surface expression of the Flores thrust (i.e. faults, folds) off Bali, Lombok and Sumbawa, (2) determine the spatial relationship between seismicity, volcano and thrust faults, (3) analyse the crustal deformation caused by the $M_w 6+$ events and (4) resolve the seismogenic structures and evaluate the coseismic rupturing during this earthquake sequence.

2 DATA SETS

High-resolution 2-D marine seismic profiles were acquired by Multi-Client Geophysical in December 2014 on board the seismic vessel Raja Elang towing a 7-km-long streamer at 7.5 m water depth and a 3200 in³ airgun source at 6.5 m depth. The shot point interval was 25 m and the record length was 9.2 s. The data was processed using a standard processing technique that includes noise suppression, common-mid point binning, velocity analysis, and pre-stack time migration. Special attention was given to enhance the low frequencies. These seismic data sets were courtesy of Multi-Client Geophysical, and have not been published elsewhere.

The earthquake data used in this study is from the USGS catalogue ($M > 4$) and the focal mechanism is from the Global Centroid Moment Tensor catalogue (GCMT, $M_w > 4$). The geographical bound applied to choose the seismicity is from 115.75° to 117.25° in longitude and from -9° to -7.5° in latitude, which covers the Lombok Island and its adjacent area. Time period for the selection of seismicity is between January 2018 and November 2019. We chose to only plot earthquakes $< 40 \text{ km}$ depth to eliminate those deep events resulting from the subduction of the Indo-Australian Plate beneath Sunda (e.g. Hall & Spakman 2015). Note that the USGS catalogue is not completely down to $M3$ in this region of the world, and the actual completeness value is likely $\sim M4$ or greater, so the earthquakes analysed in this study are predominantly $M > 4$.

3 RESULTS

3.1 Seismic interpretation and structural mapping

The term of ‘Flores thrust’ was initially used by Silver *et al.* (1983) to represent the frontal thrust of the zone of backarc thrusting north of the Flores Island. Later on, Silver *et al.* (1986) suggested that the Flores thrust of Silver *et al.* (1983) to be termed as the Flores thrust

zone and mapped a complicated zone of fault and fold structures at the eastern portion of this thrust, $\sim 300 \text{ km}$ east of Lombok. Based on the definition of Silver *et al.* (1986), we used 22 2-D seismic lines spaced at 10–20 km intervals ($\sim 2120 \text{ km}$ long in total) to interpret the subsurface structures of the Flores thrust, map its surface expression and try to resolve its western end. These lines are $\sim N-S$ trending, approximately perpendicular to the E–W striking Flores thrust and are distributed along $\sim 300 \text{ km}$ segment of the Flores thrust from the Bali basin to off Sumbawa (Fig. 1b).

In Fig. 2, three profiles (1, 2 and 3) closest to the Lombok earthquake sequence are presented. They are $\sim 55 \text{ km}$ long and have depth extending up to $\sim 6 \text{ s}$ of two-way traveltime (tw). Three principal stratigraphic units are interpreted from deep to shallow levels based mainly on the seismic facies (with reference to previous study by Foden (1983)): (1) basement, represented by chaotic, high-amplitude but poorly continuous horizons (top marked by brown horizon); (2) Unit 1, characterized by low-amplitude horizons of moderate continuity, possibly representing the Upper Miocene limestone (top marked by blue horizon); (3) Unit 2, represented by continuous horizons of alternating high and low amplitudes that onlap the Unit 1 at the northern part of the seismic profiles, representing Pliocene to present young sediments (top marked by green horizon). A gentle, landward dipping basal fault is recognized at 4.8 s at the south end of profile A and at 5.6 s at the south end of profiles B and C, extending 30–35 km northward into the foreland basin. Overlying the basal faults deform units affected by thrusts (mapped in black and red) and folds.

The high angle structures are mostly the imbricate thrusts while the low angle structure is the basal fault (see also Silver *et al.* 1983, 1986). Both the basal thrust and imbricate thrusts in this area are blind, dying out at various depths ($> 0.5 \text{ s}$) below the seabed (Fig. 2). The surface expression of the Flores thrust is a wide zone (~ 10 – 20 km) of folds, without day-lighting faults, despite the presence of a few minor, rootless normal faults (up to 2 s depth) on the back-limb of an anticline (at 8 km in profile 2). Incipient folding is observed in the foreland region, with minimal or negligible effect on the seafloor (Fig. 2). The basal fault and frontal faults in the foreland (i.e. red thrusts) appear to be active while those lying beneath Unit 1 or 2 in the hinterland (i.e. black thrusts) are inactive. We infer that the initial deformation of the Flores thrust must have been south of our seismic profiles (e.g. beneath Lombok), leading to the partial uplift of Lombok and the subsidence of the Bali basin over the old continental sediments (i.e. basement and Unit 1), and has propagated further northwards, generating folds/thrusts within recently deposited sediments Unit 2.

Westward in the Bali Basin, structural interpretation on two 2D seismic profiles (Fig. 3) shows very less deformation compared to off Lombok (Fig. 2). There are two minor, mostly buried folds observed on profile 4 (at 10–20 km distance) and only one on profile 3 (at 5 km distance), the westernmost line in this study (Fig. 1b). These folds appear to be at the initial growth stage as indicated by the lack of seafloor expression and the absence of obvious bedding-cut thrust faults. This is in contrast to the fold and thrust structures off Lombok Island where both features are well developed (Fig. 2). However, similar to off Lombok Island, the seafloor expression of the Flores thrust off Bali Island is also dominated by folds, not faults.

Further eastward offshore Sumbawa, the Flores thrust zone is marked by 1–2 large, north-vergent, thrust faults breaking through the seafloor (i.e. at 46 km on profile 6, 20 and 25 km on profile 7 in Fig. 4). Together with their hanging-wall folds, these large thrusts have generated 1–2 remarkable fault scarps with height up to 1 s

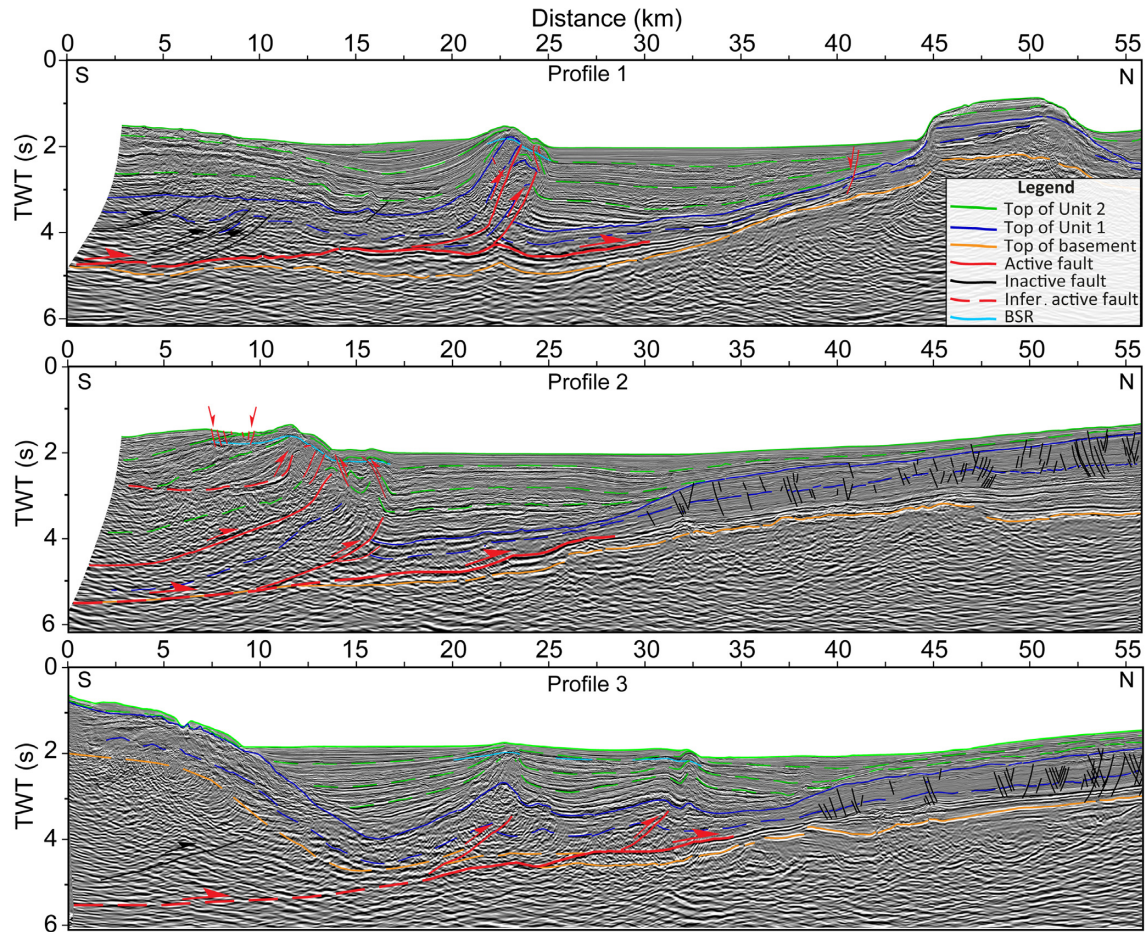


Figure 2. Three 2-D seismic profiles (1, 2 and 3) across the Flores thrust off Lombok superimposed with structural interpretation (vertical to horizontal exaggeration: 1:3 at 1.5 km s^{-1}). For the location of seismic lines, see Fig. 1(b). BSR is the Bottom-Simulating Reflector. BSR roughly parallels the seafloor reflection and represents the hydrate stability zone with gas hydrate saturated sediments above and free gas saturated sediments below (Singh *et al.* 1993). The uninterpreted seismic profiles are available in the supplementary material.

(Fig. 4), indicative of strong structural deformation. This is in contrast to the fold-dominated seafloor expression off Bali and Lombok Islands (Figs 2 and 3). The inset image shows a zone of intensive deformation with highly folded stratigraphic sequences, ~ 10 high-angle thrust faults over just ~ 3 km distance and a remarkable frontal thrust breaking through the seafloor. These observations indicate an increasing deformation eastwards from off Bali to off Sumbawa, which is compatible with the recent GPS measurement that shows an eastward increasing convergence rate along the Flores thrust in this region (Koulali *et al.* 2016).

Profile 6 extends much further south compared to other seismic profiles (Fig. 1b) and allows more bathymetry and seismic image off Sumbawa to be recorded (Fig. 4). It is intriguing to observe that the seafloor at 10–20 km distance dips southward to the island, rather than northward to the sea as expected from most offshore slope. Similarly, the top of basement near the island (at 5–25 km distance) and north of the foreland basin (at 50–60 km) also dips southward. We estimated $2\text{--}3^\circ$ dip angle for the seafloor near the island using 1.5 km s^{-1} seismic velocity for seawater. As the depth from the seafloor to the top of basement is roughly constant at 10–20 km and 50–60 km in this profile, we therefore consider the dip of basement equivalent to the southward dipping seafloor, that is $2\text{--}3^\circ$. The cause of this and its implication on the regional tectonics are discussed in the Section 4.6.

Fig. 1(c) presents our seafloor mapping of the Flores thrust zone, which shows fold-dominated surface structures off Lombok and Bali Islands (see Figs 2 and 3) whereas a few daylight thrusts are observed off Sumbawa (see Fig. 4). These structures essentially trend E–W with a minor change to WNW–ESE towards the Bali basin where they seem to diminish (i.e. westward extension of the backarc thrust, Widiyantoro & Fauzi 2005). This result slightly contrasts with the previous work of Koulali *et al.* (2016) that suggests that the Flores thrust extends all the way to East Java through the Bali basin according to the onshore GPS measurements. We attribute this discrepancy to either structural termination, that is the Flores thrust terminates westward in the Bali basin, or structural segmentation, that is one segment of the Flores thrust ends in the Bali basin and another segment exists further west in East Java. It is also possible that there are thrust structures lying further south of our seismic profiles and even beneath Bali Island (Figs 1b and c). So detailed multibeam mapping combined with seismic interpretation is needed to resolve the precise trace of the Flores–Wetar thrust system.

3.2 Seismicity

All the earthquakes < 40 km depth occurred on the Lombok Island and its adjacent area from January 2018 to November 2019 (Fig. 5)

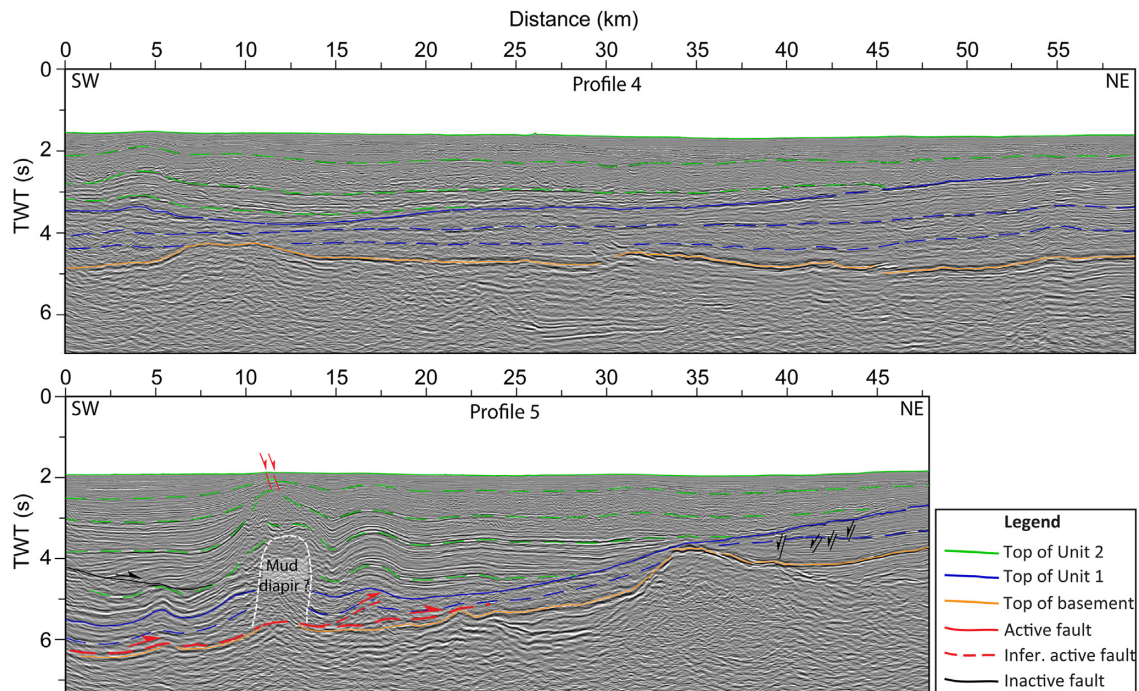


Figure 3. Two 2-D seismic profiles 4 and 5 from the Bali basin superimposed with structural interpretation (vertical to horizontal exaggeration: 1:3 at 1.5 km s^{-1}). For the location of seismic lines, see Fig. 1(b). The interpreted structures suggest less deformation in the Bali basin and possibly western end of the Flores thrust as indicated by the minor, largely buried fold at 5 km on profile 3. The uninterpreted seismic profiles are available in the supplementary material.

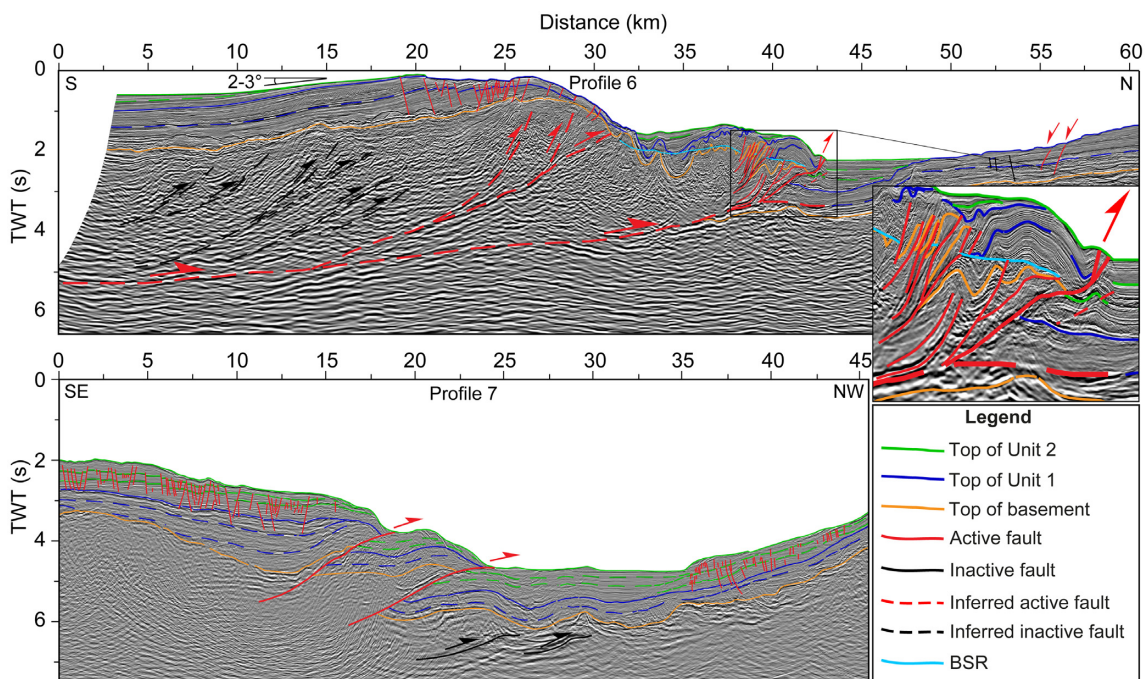


Figure 4. Two 2-D seismic profiles 6 and 7 across the Flores thrust off Sumbawa superimposed with structural interpretation (vertical to horizontal exaggeration: 1:3 at 1.5 km s^{-1}). For location of seismic lines, see Fig. 1(b). Note the southward dipping seafloor and top of basement on the profile 6 (10–20 km), which is interpreted to result from the back rotation of thrusting, slip partition and/or tectonic bending related to the loading of the Sumbawa island. The uninterpreted seismic profiles are available in the supplementary material.

are categorized into three groups based on their occurrence time: pre-Lombok sequence (purple, 1st January 2018–27th July 2018), Lombok sequence (green, 28th July 2018–19th August 2018) and post-Lombok sequence (blue, 20th August–30th November 2019).

The pre-Lombok sequence is composed of only two earthquakes located in the northwest and northeast of the island, respectively (Fig. 5a). In contrast, the post-Lombok sequence comprises 72 events that were broadly distributed in the north of the island with

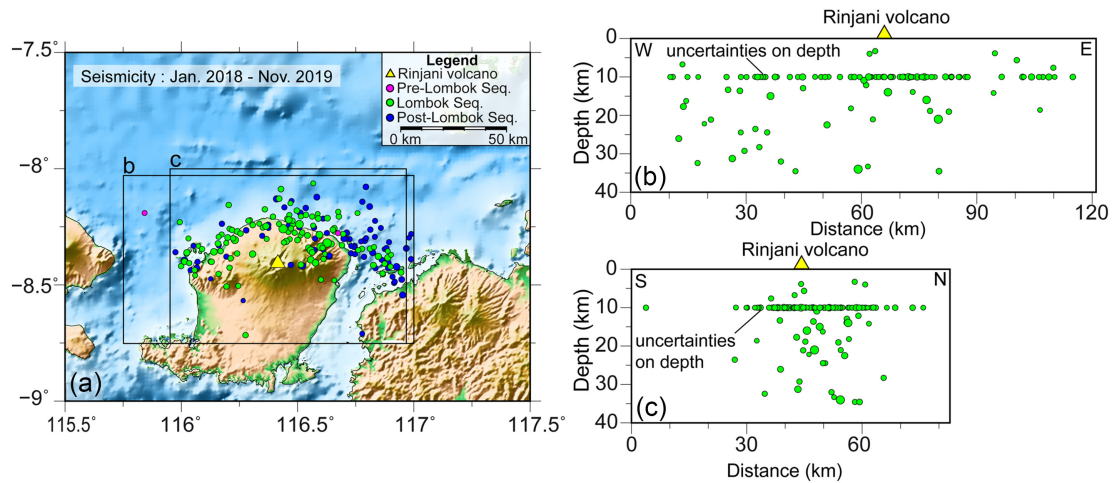


Figure 5. (a) Earthquakes (USGS catalogue) on the Lombok Island and its vicinity from January 2018 to November 2019. Black rectangles are the regions of plotted seismicity along longitude (W–E) and along latitude (N–S). (b) A W–E cross-section of seismicity. (c) A N–S cross-section of seismicity. Note the earthquakes with unresolved depth are located at 10 km by the USGS catalogue.

a slight concentration in the east and northeast, perhaps suggesting an eastward and northeastward migration of seismicity following the Lombok sequence.

To examine the spatial relationship between the Lombok sequence and the Rinjani volcano, we plotted two cross-sections of seismicity through the volcano along longitude and latitude (Figs 5b and c). Along strike, the Lombok seismicity is within ~50–60 km of the volcano, with slight more events in the west (Fig. 5b). However, along latitude NS profile the seismicity is mostly distributed within ~30 km north of volcano. The scatter of seismicity on cross-sections is possibly due to the poorly resolved earthquake locations in the used data sets.

The magnitude–time (M – T) plot in Fig. 6(a) shows that prior to the Lombok sequence, seismicity on Lombok Island was low, that is only two $M4+$ events occurred in January–June 2018. In contrast, the seismicity on Lombok Island following this sequence remained very high with 46 $M4+$ earthquakes in a month (Fig. 6a). The subsequent seismicity steadily decreased until June 2019. From July to November 2019, only two $M4+$ earthquakes occurred on Lombok Island, which is considered to be similar to the pre-Lombok sequence. The aftershocks of this striking earthquake sequence appear to have lasted >10 months from late August 2018 to June 2019 before the seismicity resumes the pre-Lombok sequence level in July 2019, which is a rather long time period compared to days-to-weeks duration of many volcanic earthquake swarms (e.g. Benoit & McNutt 1996; Llenos & van der Elst 2019).

Furthermore, the Lombok earthquake sequence did not occur regularly with a similar number of events on each day. Instead, it seems to comprise three individual earthquake clusters that started on 28th July, 5th and 19th August, respectively (Fig. 6b). Each cluster is characterized by 1–2 $M_w > 6$ events and followed by dozens of smaller events within 1–2 d (Fig. 6b). The time period between these clusters is characterized by approximately one event per day (Fig. 6b).

3.3 Coseismic crustal deformation

After the Lombok earthquake sequence, Geospatial Information Authority of Japan (GSI) applied interferometric analysis using ALOS-2/PALSAR-2 data to measure the crustal deformation caused

by 3 $M_w 6+$ earthquakes (Fig. 7). The InSAR result indicates that the crustal deformation essentially occurred in the northern part of the island with minor offshore component (Fig. 7). Near the northwest margin of the island, the maximum vertical deformation is measured as high as ~36 cm (Fig. 7b), caused by the 5th August $M_w 6.9$ event. A similar InSAR study carried out by Ganas *et al.* (2018) estimated a 28 cm maximum vertical movement related to the combined effects of the 28th July $M_w 6.4$ event and the 5th August $M_w 6.9$ event at the similar site (Fig. 7b).

Given the relatively long distance (>30 km) between southernmost mapped fold and the island (Fig. 7), the offshore component of deformation inferred from InSAR measurement has probably not reached the folds and underlying thrusts imaged on our seismic profiles offshore (Fig. 2), but has likely been limited to the slope. Based on these observations, we propose that the coseismic deformation during the Lombok sequence uplifted the northern part of the island and its northern slope, but did not rupture offshore.

4 DISCUSSION

4.1 Type of earthquakes

The Lombok earthquake sequence occurred mainly on the north side of the Rinjani volcano (Figs 1b and 5), contrasting with most volcanic earthquakes which commonly occur around a volcano (e.g. White & McCausland 2016). The Lombok sequence include 111 $M4+$ earthquakes with four events $>M_w 6$, which are much larger than most volcanic earthquakes that do not exceed $M2$ or 3 (Zobin 2001). Moreover, the focal mechanism of the Lombok seismicity shows a relatively consistent direction of fault slip (i.e. N–S, Fig. 1c), rather than a gradual change to mimic the radiation pattern of magma intrusion. Therefore, these events are likely not pure volcanic earthquakes. However, the majority of the Lombok seismicity occurs within ~30 km north and ~50–60 km west and east of the Rinjani volcano, not further west to Bali or east to Sumbawa (Figs 5b and c). If these events were purely of tectonic origin, such an apparently concentrated earthquake distribution would be difficult to explain. Putting all these features together, we propose that the Lombok earthquakes were probably resulted from the interaction between volcanic and tectonic activities.

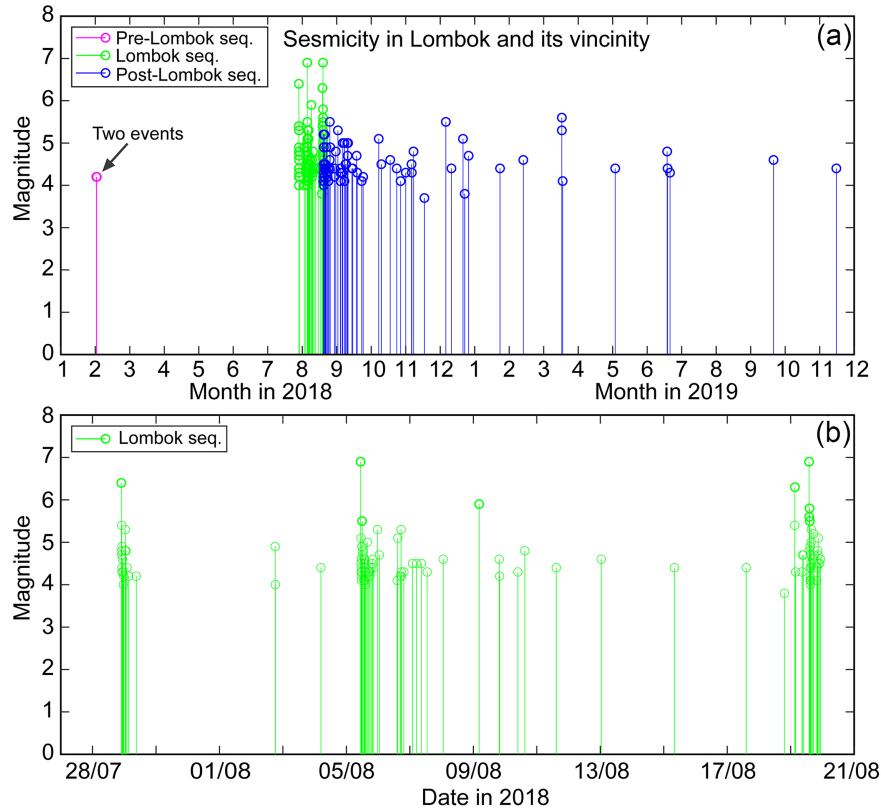


Figure 6. Magnitude–time (M – T) plot of $M > 4$ seismicity on the Lombok Island area. (a) Earthquakes between January 2018 and November 2019. (b) Lombok earthquake sequence from 28th July to 19th August 2018.

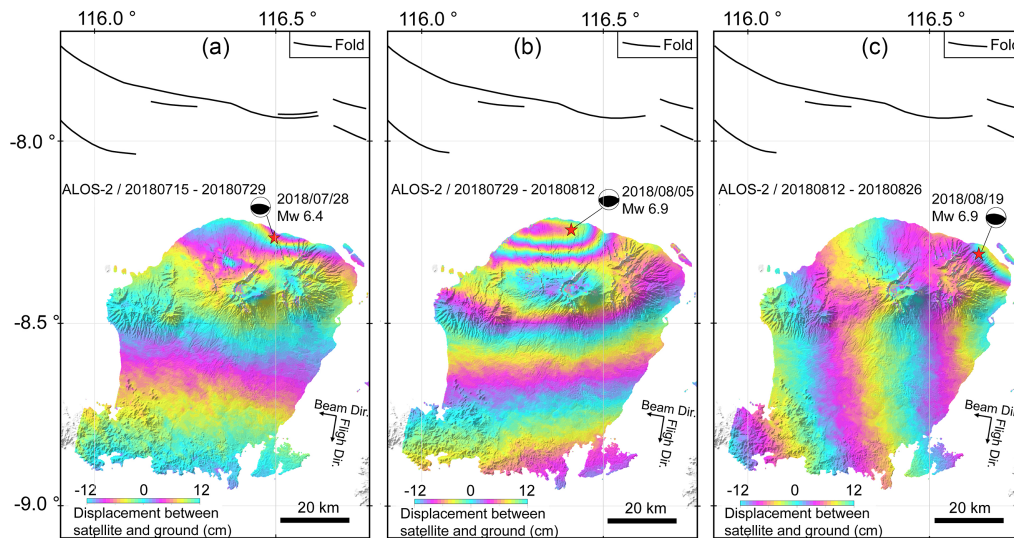


Figure 7. ALOS-2 SAR interferogram showing LOS deformation on Lombok Island, Indonesia for the 2018/07/28 M_w 6.4, 2018/08/05 M_w 6.9 and 2018/08/19 M_w 6.9 earthquakes. The InSAR image is downloaded from <https://www.gsi.go.jp/cais/topic180731-index-e.html>. The focal mechanisms are from the USGS catalogue.

4.2 2-D cross-section across Lombok

A topography profile across the Lombok, the backarc basin and south Sundaland (see Fig. 1b for location) is integrated with the results of our structural interpretation (Fig. 2), published information about the Rinjani volcano (Métrich *et al.* 2017) and imaged crustal structure across the central Sunda margin (Kopp *et al.* 2001) to

create a schematic model to illustrate the regional tectonic elements (Fig. 8a). Based on the interpreted structures off Lombok (Figs 1c and 2), the Lombok earthquakes (<40 km) beneath the island and the thrust focal mechanism (average 25° , GCMT catalogue, Figs 8b and c), we extend the Flores thrust further southward beneath the island (Fig. 8a). The Moho is at ~ 23 km depth with its geometry reflecting the bending. Two magma chambers beneath the Rinjani

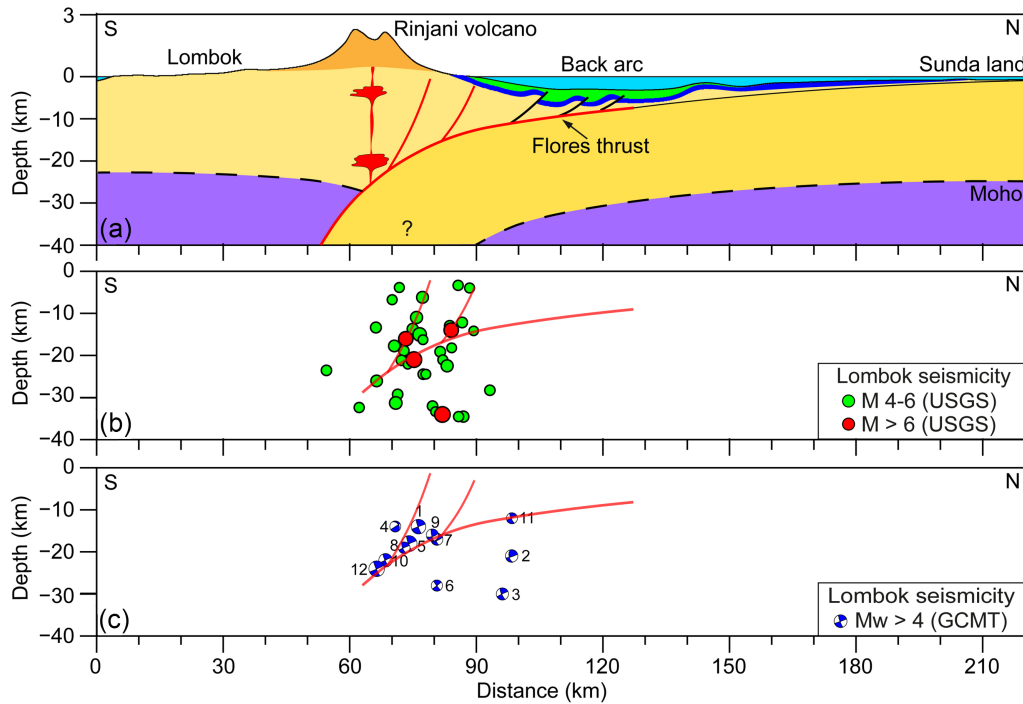


Figure 8. Tectonic model of the Lombok seismicity. For location of the topographic profile and spatial range of seismicity (see Fig. 1b). The colour scheme and associated stratigraphic units in the model correspond to the structural interpretation in Fig. 2. (a) Topography across Lombok Island and backarc basin. Fault structures are approximately based on the seismic images and seismicity beneath Lombok. The topography and bathymetry are approximately exaggerated by a factor of 10. (b) Cross-section of the Lombok seismicity using the USGS catalogue. (c) Cross-section of the Lombok earthquakes using the GCMT catalogue.

volcano are placed at 20 and 5 km depth, respectively (Métrich *et al.* 2017).

Both the USGS earthquake locations and GCMT focal mechanisms are used (Figs 8b and c) to estimate the location and possible geometry of active faults beneath the island and slope. Note that the seismicity with unresolved depth (Figs 5b and c) are eliminated from the new cross-section (Fig. 8b). There is an obvious difference in the earthquake locations between the USGS catalogue and GCMT catalogue (Figs 8b and c). For instance, the GCMT catalogue shows three earthquakes (No. 2, 3, 11) north of the 90 km distance while the USGS catalogue locates most earthquakes south of the 90-km distance. The locations of four $M > 6$ events (red) from the USGS catalogue are also inconsistent with those from the GCMT catalogue (No. 1, 5, 12), and GCMT catalogue does not contain the 19th August M_w 6.3 event. In addition, the USGS earthquakes are of wider depth ranging between 5 and 35 km while the GCMT earthquakes have a slightly narrower range of depths, that is 10–30 km. Since both catalogues use global seismological network the earthquake locations would have large uncertainties. The discrepancy between the two earthquake catalogues (Figs 8b and c) reflects the uncertainties and even errors in the earthquake locations.

In our model, the thrust faults and related folds offshore are drawn largely based on our structural interpretation of marine seismic profiles (Figs 2 and 8a) while the structures beneath the island are inferred from the Lombok seismicity. The scatter of earthquake distribution (Figs 8b and c) suggests that a network of faults, not a single one, are likely responsible, so both the basal fault and overlying imbricate thrusts (i.e. marked by red in Fig. 8a) north of the Rinjani volcano are interpreted as seismogenic structures. To simplify the model, only two high-angle faults are drawn to represent the network of imbricate thrusts. Because of the wide

range of earthquake depths (5–35 km), a gentle, constant basal detachment estimated from the frontal structures (Fig. 2) is unable to reach the deep events (>20 km), therefore we postulated an increasing basal dip southward beneath the island, forming a large ramp (Fig. 8a). Note that it is entirely possible that the relocated seismicity localizes along a single fault plane, for example basal fault, rather than a range of fault planes indicated in Fig. 8.

4.3 Nature of rupture during the Lombok earthquake sequence

Our result suggests that the offshore blind thrust faults did not rupture during the Lombok sequence (Figs 7 and 8a). There is a distinct structural variation in terms of seafloor faulting along the >800 km of backarc thrust from off Bali to off NE Wetar (Fig. 1a). In the west, we mapped a 300-km-long portion of the 450-km-long Flores thrust as a 20–40 km wide deformation zone of dominant E–W trending folds with the addition of a few faults (up to 30 km long) off Sumbawa (Fig. 1c). In contrast, 100 km eastward, Silver *et al.* (1986) using similar data sets (SeaMarc II sonar bathymetry and seismic profiles) mapped a segment of $\sim 100^\circ$ trending thrust faults and a range of NE trending cross-cut faults off Flores, some 60 km west of the 1992 tsunamigenic Flores earthquake (Beckers & Lay 1995). For the 350-km-long Wetar thrust in the east, Silver *et al.* (1983) and Breen *et al.* (1989) mapped a 1–18 km wide (westward increasing) zone of thrust faults on the seafloor, near the tsunamigenic 2004 Alor earthquake. These daylight active thrusts are interpreted to have played a key role in triggering tsunamis during the 1992 Flores earthquakes and 2004 Alor earthquake.

However, there is no tsunami triggered by the Lombok sequence, which can be attributed to a few factors, such as the relatively low earthquake magnitude ($M < 7$), concentration of epicentres and

primary crustal deformation on the island and near slope, blind nature of thrust faults off Lombok. These factors may also suggest a lower tsunami potential off Lombok and Bali compared to off Flores and Wetar, but we cannot rule out the possibility of large tsunami in the future. We noted that the active thrust faults are not buried deep off Lombok, that is slightly >0.5 s beneath the seafloor (Profile 1 and 2 in Fig. 2), it is entirely possible for the future large earthquakes ($M > 7$) occurring on these faults to rupture and uplift seafloor to generate tsunami.

4.4 Implications for fault reactivity induced by volcanism

It is intriguing that the inferred source structures for the 2018 Lombok sequences are deep-rooted imbricate thrusts and basal fault (Fig. 8a, similar to black thrusts in Fig. 2), not the frontal active thrusts (red thrust faults in Fig. 2). As the Rinjani volcano is very active, the forceful ascent of magmatic fluids and gas might have migrated through the existing fault networks of the Flores thrust (i.e. southward extension beneath Lombok) to smooth the faults, triggering seismicity. A similar scenario is proposed in an active continental rift in New Zealand where faults on the periphery of dry, mafic crust are weakened by the movement of hot fluids as a driver for the lower-crustal earthquakes (Reyners *et al.* 2007). Secondly, during magmatic activity, the resulting pressure surge propagates through an existing fault mesh to deform the brittle crust in episodes of volcanic unrest (Hill *et al.* 2002). Pressure changes in the magma chamber could nudge the stress field on the neighbouring Flores thrust closer to the condition for brittle failure, eventually inducing seismic slip.

Previous studies examined the mutual triggering of volcanic events and earthquakes in Italy, California and Japan over the past few hundred years and found that pairs of events usually occurred within 10 yr or less at distances of a few hundred km (Hill *et al.* 2002). The last 15 yr (2004–2019) has seen four eruptions from the Rinjani volcano (last one in 2016) with considerable volumes of erupted ash, lava flows or both, while within ~ 40 yr (1965–2003) before this period only three eruptions were recorded (ref. Smithsonian Institution). It seems that there is an increasing activity on the Rinjani volcano and it is possible that the Lombok earthquake sequence is partially caused by one or a series of volcanic events in the past decade or so.

Previous authors used scaled analogue models to show that the early thrusts are steepened and rotated to very steep dips, becoming inactive and effectively forming part of the backstop (e.g. Wu & McClay 2011). Our study highlights the possible role of magmatic activity in reactivating the old, perhaps inactive faults to produce earthquakes. Additional attention needs to be taken in future studies to evaluate seismic hazards related to early thrust faults adjacent to active volcanoes.

4.5 Mechanism of the Flores backarc thrust

It remains unclear why the backthrusts have developed in the backarc along the east Sunda arc (Hamilton 1979; Silver *et al.* 1983, 1986; Breen *et al.* 1989; this study), but are generally present in the forearc region along the Andaman–Sumatra segment of the Sunda arc (Chauhan *et al.* 2009; Singh *et al.* 2010, 2013; Mukti *et al.* 2012). One of the principal mechanisms put forward to explain the origin of the Flores backthrust is the stress transfer through the rigid arc-block due to change from the subduction in the west to collision in the east (Silver *et al.* 1983; ten Brink *et al.* 2009). We

noted that in the Andaman–Sumatra segment, there is a remarkable, continuous fore-arc high, that is ridges, islands (e.g. Nias, Siberut), which parallels to the Sumatra subduction zone. The backthrust in the Andaman–Sumatra segment are formed northeast of this forearc high, similar to the Flores thrust that are developed north of the volcanic arc (e.g. Lombok, Sumbawa and Flores). As such, we interpret that the forearc high acts as a rigid arc-block to transfer the stress from the oceanic subduction to the forearc region to generate the back-thrust along the Andaman–Sumatra segment of the Sunda arc.

4.6 Possible implications for the subduction initiation

The $2\text{--}3^\circ$ southward dip of the seafloor and the basement north of Sumbawa on profile 6 (Fig. 4) is comparable to the $3\text{--}4^\circ$ northeastward dip of the lower plate along the Sumatra oceanic subduction (Qin & Singh 2018). It seems that the build-up of the volcanic island has caused gravitational loading to bend the underlying stratigraphic sequence (Unit 1, 2 and basement), leading to the development of southward dipping thrusts beneath the islands (at $25\text{--}30$ km in profile 6) that has propagated northward forming trench-like basins along the Flores thrust.

Pysklywec (2001) shows that a reversal of subduction polarity can happen during continental collision if the subducting mantle lithosphere is prone to detach or undergo symmetric plate consumption with steepening and possible rollover. Here the east Sunda arc is driven northward by the Indo-Australian subduction (e.g. Koulali *et al.* 2016) and will eventually collide with the Sunda continental margin, similar to what is happening at the continent-arc collision along the Timor trough (Audley-Charles 2004; Shulgin *et al.* 2009). The resultant arc-continent collision will tend to block, even stop the northward oceanic subduction. It is therefore possible for the existing Flores thrust to act as a weak zone to facilitate the southward continent subduction beneath the arc as subduction initiation, which may eventually lead to a complete subduction reversal. Our model indicates the basal fault of the Flores thrust has potential to develop a southward subduction (Fig. 8a).

5 CONCLUSIONS

Combined marine seismic reflection, seismicity and InSAR measurements have allowed us to investigate the nature of rupture onshore and offshore during the 2018 Lombok seismicity of ~ 110 $M 4+$ events in Indonesia. The Lombok earthquakes are all shallow thrust events with depth <40 km, and have essentially occurred along the deep-rooted basal fault and imbricate thrusts associated with the Flores thrust beneath the island of Lombok and its nearshore. The blind nature of the Flores thrust (i.e. surface structures represented by folds) offshore north of Lombok, the onshore and nearshore dominated epicentres of the seismicity, the onshore-concentrated major crustal deformation and the long distance (>30 km) between the InSAR measured maximum vertical deformation (~ 36 cm) caused by the August 5th M_w 6.9 event on the northwest margin of the island and the southernmost mapped fold and underlying thrust offshore suggest that the majority of coseismic slip was probably accommodated by slip on the subsurface thrusts, lifting the north of the island and its slope area, but not rupturing the blind thrusts offshore. Although the blind nature of the Flores thrust off Bali and Lombok suggests a lower tsunami potential in this region compared to off Flores and Wetar, a future large earthquake ($M > 7$) could still occur on these blind thrusts to uplift

the seafloor to trigger a large tsunami. The proximity of the Rinjani volcano and thrust earthquakes implies that two mechanisms might have been involved in re-activating the existing thrusts and triggering the Lombok sequence: (1) magmatic fluids and gas migrating along the Flores thrust to weaken the faults; (2) the pressurization of a magma chamber nudging the stress field on the Flores thrust closer to brittle failure.

ACKNOWLEDGEMENTS

We thank Robert Hall and Belle Philibosian for their thorough reviews that helped to improve the paper significantly. Discussions with Kyle Bradley were extremely useful. The seismic reflection data for this study was provided by Multi-Client Geophysical for scientific research. The study leading to these results has received funding from the European Research Council under the European Union's Seventh Framework Programme (FP7/2007-2013)/ERC Advance Grant agreement n° 339442_TransAtlanticILAB. Figures 1 and 5 are plotted using Generic Map Tools (Wessel *et al.*, 2013). This is IGP contribution No. 4105.

REFERENCES

- Audley-Charles, M., 2004. Ocean trench blocked and obliterated by Banda forearc collision with Australian proximal continental slope, *Tectonophysics*, **389**(1–2), 65–79.
- Beckers, J. & Lay, T., 1995. Very broadband seismic analysis of the 1992 Flores, Indonesia, earthquake (Mw = 7.9), *J. geophys. Res.*, **100**(B9), 18 179–18 193.
- Benoit, J.P. & McNutt, S.R., 1996. Global volcanic earthquake swarm database and preliminary analysis of volcanic earthquake swarm duration, *Ann. Geophys.*, **39**(2), 221–229.
- Breen, N.A., Silver, E.A. & Roof, S., 1989. The Wetar back arc thrust belt, eastern Indonesia: the effect of accretion against an irregularly shaped arc, *Tectonics*, **8**(1), 85–98.
- Chauhan, A.P. *et al.*, 2009. Seismic imaging of forearc backthrusts at northern Sumatra subduction zone, *Geophys. J. Int.*, **179**(3), 1772–1780.
- Ekström, G., Nettles, M. & Dziewoński, A., 2012. The global CMT project 2004–2010: centroid-moment tensors for 13,017 earthquakes, *Phys. Earth planet. Inter.*, **200**, 1–9.
- Foden, J., 1983. The petrology of the calcalkaline lavas of Rindjani volcano, east Sunda arc: a model for island arc petrogenesis, *J. Petrol.*, **24**(1), 98–130.
- Ganas, A., Tsironi, V. & Valkaniotis, S., 2018. A preliminary report on the 2010 Lombok region - Indonesia earthquakes National Observatory of Athens, Institute of Geodynamics.
- Hall, R. & Spakman, W., 2015. Mantle structure and tectonic history of SE Asia, *Tectonophysics*, **658**, 14–45.
- Hamilton, W.B., 1979. *Tectonics of the Indonesian Region*, USGS.
- Hill, D.P., Pollitz, F. & Newhall, C., 2002. Earthquake-volcano interactions, *Phys. Today*, **55**(11), 41–47.
- Hutchison, C.S., 1976. Indonesian active volcanic arc: K, Sr, and Rb variation with depth to the Benioff zone, *Geology*, **4**(7), 407–408.
- Kopp, H., Flueh, E.R., Klaeschen, D., Bialas, J. & Reichert, C., 2001. Crustal structure of the central Sunda margin at the onset of oblique subduction, *Geophys. J. Int.*, **147**(2), 449–474.
- Koulali, A. *et al.*, 2016. Crustal strain partitioning and the associated earthquake hazard in the eastern Sunda-Banda arc, *Geophys. Res. Lett.*, **43**(5), 1943–1949.
- Lavigne, F. *et al.*, 2013. Source of the great AD 1257 mystery eruption unveiled, Samalas volcano, Rinjani Volcanic Complex, Indonesia, *Proc. Natl. Acad. Sci.*, **110**(42), 16 742–16 747.
- Llenos, A.L. & van der Elst, N.J., 2019. Improving earthquake forecasts during swarms with a duration model, *Bull. seism. Soc. Am.*, **109**(3), 1148–1155.
- Lüschen, E., Müller, C., Kopp, H., Engels, M., Lutz, R., Planert, L., Shulgin, A. & Djajadihardja, Y., 2011. Structure, evolution and tectonic activity of the eastern Sunda forearc, Indonesia, from marine seismic investigations, *Tectonophysics*, **508**(1–4), 6–21.
- Mukti, M.M.r., Singh, S.C., Deighton, I., Hananto, N.D., Moeremans, R. & Permana, H., 2012. Structural evolution of backthrusting in the Mentawai Fault Zone, offshore Sumatran forearc, *Geochem. Geophys. Geosyst.*, **13**(12), Q12006.
- Métrich, N. *et al.*, 2017. New insights into magma differentiation and storage in holocene crustal reservoirs of the lesser Sunda arc: the Rinjani–Samaras volcanic complex (Lombok, Indonesia), *J. Petrol.*, **58**(11), 2257–2284.
- Pysklywec, R.N., 2001. Evolution of subducting mantle lithosphere at a continental plate boundary, *Geophys. Res. Lett.*, **28**(23), 4399–4402.
- Qin, Y. & Singh, S.C., 2018. Insight into frontal seismogenic zone in the Mentawai locked region from seismic full waveform inversion of ultralong offset streamer data, *Geochem. Geophys. Geosyst.*, **19**(11), 4342–4365.
- Reyners, M., Eberhart-Phillips, D. & Stuart, G., 2007. The role of fluids in lower-crustal earthquakes near continental rifts, *Nature*, **446**(7139), 1075.
- Shulgin, A. *et al.*, 2009. Sunda-Banda arc transition: incipient continent-island arc collision (northwest Australia), *Geophys. Res. Lett.*, **36**(10), doi:10.1029/2009GL037533.
- Sigl, M. *et al.*, 2014. Insights from Antarctica on volcanic forcing during the Common Era, *Nat. Climate Change*, **4**(8), 693–697.
- Silver, E.A., Breen, N.A., Prasetyo, H. & Hussong, D.M., 1986. Multibeam study of the Flores backarc thrust belt, Indonesia, *J. geophys. Res.*, **91**(B3), 3489–3500.
- Silver, E.A., Reed, D., McCaffrey, R. & Joyodiwiryo, Y., 1983. Back arc thrusting in the eastern Sunda arc, Indonesia: a consequence of arc-continent collision, *J. geophys. Res.*, **88**(B9), 7429–7448.
- Singh, S.C., Hananto, N.D., Chauhan, A.P., Permana, H., Denolle, M., Hendriyana, A. & Natawidjaja, D., 2010. Evidence of active backthrusting at the NE Margin of Mentawai Islands, SW Sumatra, *Geophys. J. Int.*, **180**(2), 703–714.
- Singh, S.C., Minshull, T.A. & Spence, G.D., 1993. Velocity structure of a gas hydrate reflector, *Science*, **260**(5105), 204–207.
- Singh, S.C., Moeremans, R., McArdle, J. & Johansen, K., 2013. Seismic images of the sliver strike-slip fault and back thrust in the Andaman-Nicobar region, *J. geophys. Res.*, **118**(10), 5208–5224.
- ten Brink, U.S., Marshak, S. & Bruña, J.-L.G., 2009. Bivergent thrust wedges surrounding oceanic island arcs: insight from observations and sandbox models of the northeastern Caribbean plate, *Bull. geol. Soc. Am.*, **121**(11–12), 1522–1536.
- Usna, I., Tjokrosapetro, S. & Wiryosujono, S., 1979. Geological interpretation of a seismic reflection profile across the Banda Sea between Wetar and Buru islands, *Bull. Geol. Res. Dev. Centre*, **1**, 7–15.
- Vidal, C.M. *et al.*, 2015. Dynamics of the major plinian eruption of Samalas in 1257 AD (Lombok, Indonesia), *Bull. Volcanol.*, **77**(9), 73.
- Wessel, P., Smith, W.H.F., Scharroo, R., Luis, J.F. & Wobbe, F., 2013. Generic Mapping Tools: Improved version released, *EOS Transactions*, **9**, 409–410.
- White, R. & McCausland, W., 2016. Volcano-tectonic earthquakes: a new tool for estimating intrusive volumes and forecasting eruptions, *J. Volc. Geotherm. Res.*, **309**, 139–155.
- Widiyantoro, S. & Fauzi, 2005. Note on seismicity of the Bali convergent region in the eastern Sunda Arc, Indonesia, *Aust. J. Earth Sci.*, **52**(3), 379–383.
- Wu, J.E. & McClay, K.R., 2011. Two-dimensional analog modeling of fold and thrust belts: Dynamic interactions with syncontractional sedimentation and erosion, in McClay, K.R., Shaw, J. & Suppe, J., eds *Thrust Fault-Related Folding*, pp. 301–333, Vol. **94**, American Association of Petroleum Geologists Memoir.
- Zobin, V.M., 2001. Seismic hazard of volcanic activity, *J. Volc. Geotherm. Res.*, **112**(1–4), 1–14.

SUPPORTING INFORMATION

Supplementary data are available at [GJI](#) online.

Figure S1. Uninterpreted 2-D seismic profiles 1, 2 and 3, for locations see Fig. 1(b).

Figure S2. Uninterpreted 2-D seismic profiles 4 and 5, for locations see Fig. 1(b).

Figure S3. Uninterpreted 2-D seismic profiles 6 and 7, for locations see Fig. 1(b).

Please note: Oxford University Press is not responsible for the content or functionality of any supporting materials supplied by the authors. Any queries (other than missing material) should be directed to the corresponding author for the paper.